Radiation Physics and Chemistry 208 (2023) 110885

Contents lists available at ScienceDirect

Radiation Physics and Chemistry

journal homepage: www.elsevier.com/locate/radphyschem

γ–radiolytic degradation of rosuvastatin in the air–saturated aqueous solution

Leo Mandić [a], Marijana Pocrnić [b], Nives Galić [b], Branka Mihaljević [a], Iva Džeba [a,*]

[a] Radiation Chemistry and Dosimetry Laboratory, Division of Materials Chemistry, Ruđer Bošković Institute, Bijenička cesta 54, 10000, Zagreb, Croatia
[b] Department of Chemistry, Faculty of Science, University of Zagreb, Horvatovac 102a, 10000, Zagreb, Croatia

ARTICLE INFO

Handling Editor: Dr. Jay Laverne

Keywords:
Wastewater treatment
Rosuvastatin
γ-radiolysis
Laser flash photolysis
High-resolution mass spectrometry
Rate constant
Mechanism

ABSTRACT

Widespread environmental occurrence and persistence of pharmaceuticals have attracted great concern due to their incomplete removal by conventional wastewater treatment technologies. The use of radiation technology has proven to be a good and successful alternative where highly reactive species lead to high degradation level of pharmaceuticals. Among the most commonly prescribed pharmaceuticals is rosuvastatin (ROSU), cholesterol-lowering agent, which has been detected as a contaminant in wastewater and natural waters. The aim of the present study was to investigate the γ-radiolytic degradation of ROSU in aqueous solutions under different conditions. The focus was given to the most applicable conditions, the degradation of ROSU in air, where dominant reactions of $^{\bullet}$OH radicals with ROSU are expected. Therefore, the reaction rate constant of ROSU with $^{\bullet}$OH radicals ($2.15 \pm 0.07 \times 10^{10}$ M^{-1} s^{-1}) was determined by laser flash photolysis. By combined γ-radiolysis and mass spectrometry study, the reaction mechanism of radiation degradation of ROSU was proposed and the radiolytic products were identified.

1. Introduction

The widespread presence and persistence of pharmaceuticals in the aquatic environment has caused great concern worldwide, as they pose a potential threat to ecosystems and public health (Akhtar et al., 2015; Coimbra et al., 2021; Cuerda-Correa et al., 2019; Gadipelly et al., 2014; Golovko et al., 2014; Kanakaraju et al., 2018; Massima Mouele et al., 2021; Wang and Wang, 2016). Therefore, monitoring the levels of pharmaceuticals in wastewater and surface waters and finding effective methods to remove them are of great importance. One such promising method is γ-irradiation, which is expected to lead to high pharmaceutical degradation due to reactions with highly reactive species formed *in situ* during water radiolysis (Razavi et al., 2011b). One of the most commonly prescribed pharmaceuticals for the treatment of cardiovascular diseases are the cholesterol-lowering statins (Demasi, 2018), which may end up in wastewater due to their frequent use. One of these is rosuvastatin (ROSU, Fig. 1), a pyrimidine derivative that, like other statins, acts as a competitive inhibitor of 3-hydroxy-3-methylglutaryl--coenzyme A (HMG-CoA) reductase (Azemawah et al., 2019; Luvai et al., 2012). ROSU is often referred to as "superstatin" (Iglesias and Díez, 2003) due to its ability to lower the cholesterol level in the greater extent than any other statin (Cheng, 2004). It is a compound that is not readily biodegradable and has been detected as a contaminant in wastewater and natural waters (Lee et al., 2009; Sulaiman et al., 2015). As with other statins, different methods have been used to find an efficient ROSU degradation method (Razavi et al., 2011b; Machado et al., 2015; Segalin et al., 2015; Sulaiman et al., 2015). A recent study on the γ-radiolysis of ROSU demonstrated the sensitivity of ROSU to γ-irradiation under adjusted oxidative conditions and identified six primary degradation products (Dončević et al., 2021).

The aim of the present study was to investigate the efficiency of the ionizing radiation method on the degradation of ROSU in aqueous solutions under different irradiation conditions: different doses and dose rates, irradiation in equilibrium with air and under only oxidative or reductive conditions. The focus is given on the ROSU degradation in air as the most applicable technological conditions for the wastewater treatment, where dominant reactions of $^{\bullet}$OH radicals with ROSU can be expected. Using mass spectrometry analysis, a reaction mechanism is proposed and new radiolytic degradation products have been identified. Finally, the reaction rate constant of ROSU with $^{\bullet}$OH radicals is determined by the laser flash photolysis method.

* Corresponding author.
E-mail address: Iva.Dzeba@irb.hr (I. Džeba).

https://doi.org/10.1016/j.radphyschem.2023.110885
Received 11 November 2022; Received in revised form 16 February 2023; Accepted 28 February 2023
Available online 6 March 2023

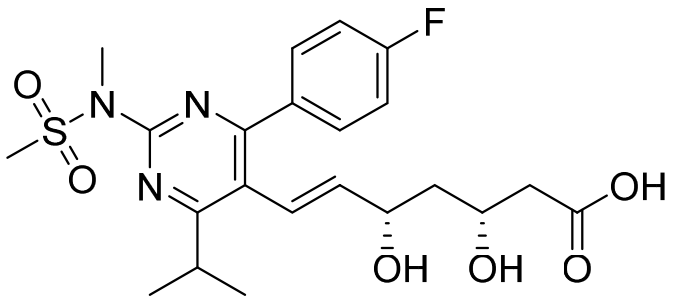

ROSU

Fig. 1. Structure of rosuvastatin.

2. Experimental

2.1. Materials

Rosuvastatin calcium (>98 %) was purchased from Acros Organics. Concentrated phosphoric acid (85 %) and all its sodium salts (>99 %) were purchased from Sigma-Aldrich. 2-mercaptopyridine-*N*-oxide from Sigma Aldrich (99 %) completely tautomerizes in polar media to *N*-hydroxypyridine-2(1*H*)-thione (HPT) (Jones and Katritzky, 1960), which is used as a source of $^{\bullet}OH$ radicals (Aveline et al., 1996; De Matteo et al., 2005). Acetonitrile (>99.9 %, HPLC grade) was purchased from Honeywell Riedel-de Haën and Carlo Erba, while 2-propanol (>99.9 %, HPLC grade) was purchased from VWR. Formic acid was purchased from Carlo Erba. Water was purified through a Millipore (Milli-Q) system. High purity nitrous oxide (N_2O) and nitrogen (N_2) were used to purge the solutions prior to the corresponding γ-radiolysis and laser flash photolysis experiments.

2.2. Reaction system preparations for γ-irradiation

Samples of the ROSU aqueous solution were irradiated using a panoramic ^{60}Co γ-source in the Radiation Chemistry and Dosimetry Laboratory of the Ruđer Bošković Institute. 0.1 mM ROSU aqueous solutions were prepared in NaH_2PO_4–Na_2HPO_4 buffer (10 mM, pH ≈ 6.5) prior to γ-radiolysis at different irradiation conditions. 3 ml of the sample solution was transferred to 5 ml glass vessels sealed with rubber septa and deaerated with N_2O or N_2, or it was irradiated in air without septa to ensure the presence of oxygen.

Radiolysis of neutral water leads to the formation of hydroxyl radicals, $^{\bullet}OH$, hydrated electrons, e_{aq}^- and hydrogen atoms, $H^{\bullet}$, with the corresponding radiation chemical yields of $G(^{\bullet}OH) = 0.28$ μmol J^{-1}, $G(e_{aq}^-) = 0.27$ μmol J^{-1} and $G(H^{\bullet}) = 0.062$ μmol J^{-1}.

To achieve the oxidation conditions, the solutions were purged with N_2O for 30 min and then irradiated with doses up to 1000 Gy. In N_2O-saturated solution (25 mM N_2O), $^{\bullet}OH$ radicals are the major reactive species as e_{aq}^- are converted into $^{\bullet}OH$ radicals ($e_{aq}^- + N_2O + H_2O \rightarrow {}^{\bullet}OH + {-}OH + N_2$; $k = 9.1 \times 10^9$ M^{-1} s^{-1}), whereas $H^{\bullet}$ react slowly with N_2O ($k = 2.1 \times 10^6$ M^{-1} s^{-1}) (Buxton et al., 1988; Spinks and Woods, 1990). The yields of reacting radicals $G(^{\bullet}OH) = 0.55$ μmol J^{-1} and $G(H^{\bullet}) = 0.062$ μmol J^{-1} correspond approximately to 90 % of $^{\bullet}OH$ radicals and 10 % of $H^{\bullet}$ atoms.

Radiolysis under reductive conditions has been studied in ROSU solutions saturated with N_2 and containing 100 mM 2-propanol, where oxidizing $^{\bullet}OH$ radicals are quantitatively scavenged by 2-propanol ($^{\bullet}OH + (CH_3)_2CHOH \rightarrow H_2O + (CH_3)_2C^{\bullet}OH$, $k = 1.2 \times 10^9$ M^{-1} s^{-1}) and form a rather inactive 2-hydroxy-2-propyl radical (Buxton et al., 1988).

In air-saturated solution $^{\bullet}H$ atoms and e_{aq}^- react with O_2 to form the pH-dependent equilibrium $HO_2^{\bullet}/O_2^{\bullet-}$ according to the reactions:

$$e_{aq}^- + O_2 \rightarrow O_2^{\bullet-} \quad (k = 1.9 \times 10^{10}\ M^{-1}\ s^{-1})$$

$$^{\bullet}H + O_2 \rightarrow HO_2^{\bullet} \quad (k = 2.1 \times 10^{10}\ M^{-1}\ s^{-1})$$

$$HO_2^{\bullet} + H_2O \rightleftarrows O_2^{\bullet-} + H_3O^+ \quad (pK_a = 4.8)$$

Therefore, $^{\bullet}OH$ radicals, e_{aq}^-, $^{\bullet}H$ atoms and $HO_2^{\bullet}/O_2^{\bullet-}$ radicals are the possible reactive intermediates in air-saturated solutions.

Dose rates were determined from recent dose mapping data obtained at the radiation facility (Majer et al., 2019), and absorbed doses were determined by chemical dosimetry based on the ethanol-chlorobenzene dosimetry system (ECB) (10 % chlorobenzene in ethanol) (Ražem and Dvornik, 1987) according to the standard ISO/ASTM 51538:2017. All irradiations were carried out at the irradiation chamber temperature of 20 °C.

2.3. Chemical analyses

The UV–Vis spectra of the reaction systems were measured using the Cary 4000 spectrophotometer equipped with the Cary PCB 150 water Peltier system (Varian, Australia). The amount of carbon bound in an organic compound or total organic carbon (TOC) was determined by the high-temperature catalytic oxidation (HTCO) method at the TOC analyzer TOC-Vcph/cpn equipped with SSM-5000 A module (Shimadzu, Japan) (Dautović et al., 2017).

HPLC analyses were performed on a KNAUER liquid chromatographic system consisting on binary pump (KNAUER K-501), vacuum degasser (KNAUER), diode-array detector (WellChrom K-2800) and ChromGate software (Version 3.1). The reaction mixtures were chromatographed on a 5 μm, 4 × 250 mm reversed-phase C_{18} ET 250/4 NUCLEOSIL (Macherey-Nagel, Düren, Germany) analytical column. Each sample run consisted of isocratic elution for 2 min with 15 % CH_3CN in 10 mM NaH_2PO_4/Na_2HPO_4 buffer (pH ≈ 7.1), gradient elution from 15 % to 60 % CH_3CN over the next 35 min and isocratic elution with 60 % CH_3CN for 8 min, at a flow rate of 1.5 mL min^{-1}. Observational wavelength was 242 nm, which corresponds to the ROSU UV–Vis absorption maximum (Fig. S1). ROSU degradation efficiency was calculated *via* ratio of the areas under the ROSU peaks in the HPLC chromatogram of the irradiated samples and the corresponding ROSU peak of the non-irradiated sample (Figs. S2–S7). All analyses were carried out at room temperature.

2.4. Laser flash photolysis

Measurements were performed on a LFP setup consisting of a Quantel Q-smart Q450 Nd:YAG laser (pulse duration – 5 ns, 10 Hz) and a LP980 Edinburgh Instruments transient absorption spectrometer. The energy of the laser pulse at the wavelength of 355 nm was set to 5 mJ (15 mJ cm^{-2}). For the kinetics measurements, static cuvettes sealed with rubber septa were used and frequently exchanged to ensure that light was not no absorbed by the photoproducts. Transient absorption spectra were measured in the flow cells. The solutions were purged for at least 30 min with N_2 prior to the measurements. All measurements were performed at 25 °C.

2.5. Identification of degradation products by HR MS

In order to identify possible structures of intermediates and propose the reaction mechanism of ROSU decomposition, samples were subjected to HR MS analysis after γ-irradiation of the air-saturated ROSU sample. Two 0.1 mM ROSU aqueous solutions were prepared in NaH_2PO_4–Na_2HPO_4 buffer (10 mM, pH ≈ 7.0). The first sample was irradiated in air ($D = 1000$ Gy, $dD/dt = 4.94$ Gy s^{-1}), while the second sample was the control sample.

The degradation products were analyzed by high pressure liquid chromatography-high resolution mass spectrometry using an Agilent

6550 Series Accurate-Mass-Quadrupole Time-of-Flight mass spectrometer coupled with an Agilent 1290 Infinity II HPLC. Chromatographic separation was performed on a Zorbax Eclipse Plus C18 column (1.8 μm, 3.0 × 50 mm). The mobile phase consisted of 0.1 % formic acid in water (A) and acetonitrile (B). Elution was performed by a gradient profile as follows: 0 min 95 % A; 15 min 5 % A; 17 min 95 % A. The flow rate was set to 0.4 mL min^{-1}, the column temperature to 40 °C, and the injection volume to 2 μL. Electrospray ionization was performed in positive mode in the mass range of 100–1000 *m/z* for MS analysis and 50–550 *m/z* for MS/MS analysis. Collision-induced dissociation was performed with collision energies (CE) of 10 V, 20 V, and 40 V. The other parameters of the mass spectrometer were optimized as follows: capillary voltage, 3500 V; sheath gas temperature, 350 °C; sheath gas flow rate, 11 L min^{-1}; drying gas temperature, 200 °C; and drying gas flow rate, 14 L min^{-1}. Nitrogen was used as drying and sheath gas.

3. Results and discussion

3.1. γ-radiolysis of ROSU reaction systems

During radiolysis of water, oxidizing (•OH radicals) and reducing species (e^-_{aq} and H•) are produced simultaneously in nearly equal amounts. This radiolytic phenomenon can be used for the degradation of contaminants and their removal from water *via* both oxidation and reduction pathways. In this study, the degradation of ROSU by γ-radiation was investigated and the results are shown in Fig. 2. As can be seen, ROSU degradation is most pronounced under oxidative conditions and is almost complete after 1000 Gy (Table S1, Fig. 2). Fig. S1 shows an absorbance decrease at about 240 nm as a function of dose in ROSU solution irradiated in air. A slight blue shift in the absorption band is observed. The degradation efficiency of 85 % obtained in equilibrium with air at a dose of 1000 Gy, relative to the initial concentration of ROSU, was close to that obtained after irradiation with the same dose under adjusted oxidizing conditions in N_2O-saturated ROSU solutions.

In both reaction systems, the •OH radicals are the main reactants, but under oxidizing conditions the radiation chemical yield is high, $G(^{\bullet}OH) = 0.55$ μmol J^{-1}, resulting in a higher degradation efficiency. Radiation generated •OH radicals have strong electrophilicity and preferentially attack the sites with high electron density, such as the phenyl ring. In addition to the side chain available for hydrogen abstraction, ROSU also has several electron donor groups (around nitrogen and fluorine) that are easily attacked by •OH radicals, leading to the cleavage of aromatic rings and subsequent formation of carboxylic acids, acetaldehyde, and other intermediates in solution. However, the TOC removal efficiency achieved after irradiation with 1 kGy was very low, which was expected due to the low dose. With an initial ROSU mass concentration of 100 mg L^{-1} and a theoretical TOC value of 52.79 mg L^{-1} before irradiation, 51.43 mg L^{-1} TOC was measured, corresponding to 2.6 % of the TOC removed after irradiation with 1 kGy. These results indicate that some ROSU degradation intermediates and low molecular weight organic acids, such as formic and acetic acids were not easily mineralized in solution at the low absorbed dose applied in this study. TOC removal could not be completed even after irradiation with the high dose of 110 kGy, after which 7.98 mg L^{-1} TOC was measured, or 84.9 % of the TOC was removed.

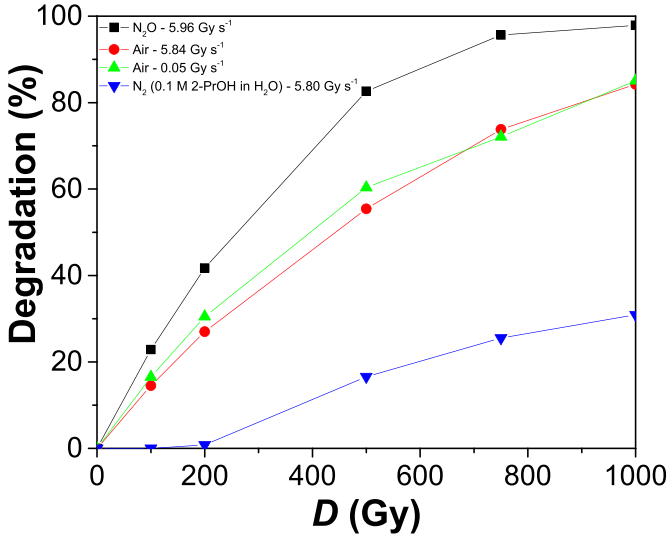

Fig. 2. ROSU degradation efficiency in H_2O (pH ≈ 6.5) at different irradiation conditions determined by HPLC.

Radiolysis under reductive conditions where only 30 % of ROSU was degraded at 1000 Gy, was much less efficient than under oxidative conditions. Nucleophilic e^-_{aq} are reactive species in reactions with aromatic organic molecules with halogen substituents, thus fluorine ions from ROSU could be released into solution after irradiation ($e^-_{aq} + RF \rightarrow RF^- \rightarrow R^{\bullet} + F^-$)(Buxton et al., 1988).

The degradation constants were calculated according to equation (1): $-\ln\left(c/c_0\right) = k_{deg} * D$, where c is the concentration of ROSU after irradiation, c_0 is the concentration of ROSU before irradiation, D is the corresponding dose, and k_{deg} is the degradation constant of ROSU (Figs. S8–S11). It is noteworthy that the degradation efficiency for air-saturated ROSU samples does not depend on the applied dose rates, which is also evident from the calculated degradation constants at different dose rates ($k_{deg} = 1.79 \times 10^{-3}$ Gy^{-1} for $dD/dt = 5.84$ Gy s^{-1} and $k_{deg} = 1.83 \times 10^{-3}$ Gy^{-1} for $dD/dt = 0.05$ Gy s^{-1}). The difference between the applied dose rates may not have been large enough to observe the difference in the degradation rate. In practice, much higher dose rates are applied as electron beam accelerators are used to achieve adequate treatment capacity of hundreds of thousands of cubic meters of wastewater per day. A twofold higher k_{deg} value ($k_{deg} = 3.87 \times 10^{-3}$ Gy^{-1}) was obtained under oxidative conditions and a fivefold lower k_{deg} value ($k_{deg} = 3.76 \times 10^{-4}$ Gy^{-1}) under reductive conditions than in air-saturated ROSU samples at the same dose rate.

3.2. Laser flash photolysis

Laser flash photolysis was used for the determination of the reaction rate constant of ROSU and •OH radicals. •OH radicals were generated by photolysis of *N*-hydroxypyridine-2-thione (HPT) in deaerated CH_3CN at 355 nm laser excitation (Scheme 1, ground state absorption spectra - Fig. S12), a method previously described by Aveline (Aveline et al., 1996) and De Matteo (De Matteo et al., 2005).

The transient absorption spectra obtained right after laser excitation of a N_2-purged CH_3CN solution of HPT alone is in a good agreement with the literature (Fig. 3) (Aveline et al., 1996; De Matteo et al., 2005), and the transient with a maximum at 490 nm is assigned to the 2-pyrithiyl radical (Scheme 1). Transient absorption spectra right after laser excitation of HPT in N_2-purged CH_3CN solution in the presence of different concentrations of ROSU clearly showed the formation of a new transient

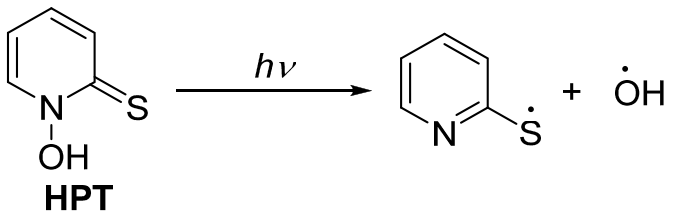

Scheme 1. Generation of •OH radicals by photolysis of HPT in CH_3CN at 355 nm.

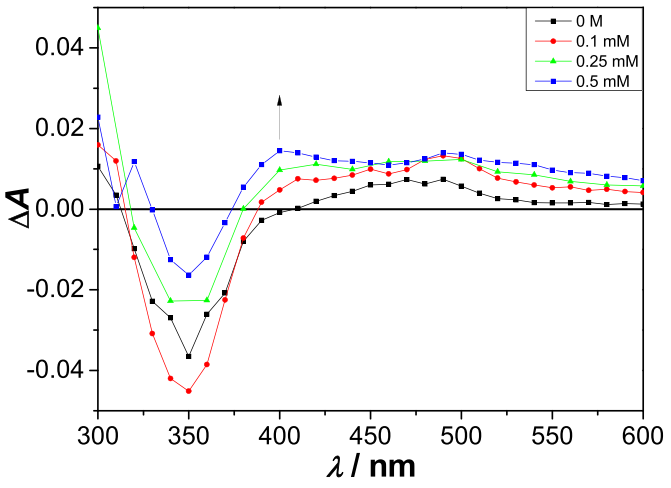

Fig. 3. Transient absorption spectra of N_2-purged CH_3CN solutions of HPT (0.1 mM) alone and in the presence of different concentrations of ROSU recorded immediately after the laser pulse. $E_{355\ nm} \approx 5$ mJ.

as a result of the reaction of ROSU and •OH radicals in the wavelength region around 400 nm, where the 2-pyrithiyl radical does not absorb (Fig. 3). It can be seen that the absorbance of the formed transient increases with increasing ROSU concentration (Fig. 3).

Apart from the evident spectral transient absorbance increase at 400 nm when ROSU is present in the HPT solution (Fig. 3), the kinetics under these conditions consist of the rapid formation of the transient within the pulse at 400 nm, which slowly decays on the nanosecond time scale (Fig. 4, Fig. S13).

The kinetics of the formation of the transient at 400 nm were determined by fitting the experimental data with the function related to the simultaneous pseudo-first order growth and decay contributions according to equation (2): $y = A \times (\exp(-t/\tau_1) - \exp(-t/\tau_2)) + y_0$, where τ_1 and τ_2 are the corresponding lifetimes, respectively. The observed pseudo-first order rate constant for transient formation monitored at 400 nm, k_{obs}, obtained from the growing component from equation (2), was plotted against the ROSU concentration (Fig. 5) according to equation (3): $k_{obs} = {}^1/_{\tau_1} = {}^1/_{\tau_0} + k_R[ROSU]$, where τ_0 is the lifetime of •OH radicals in the absence of ROSU and k_R is the reaction rate constant of ROSU and •OH radicals. From the linear plot the rate

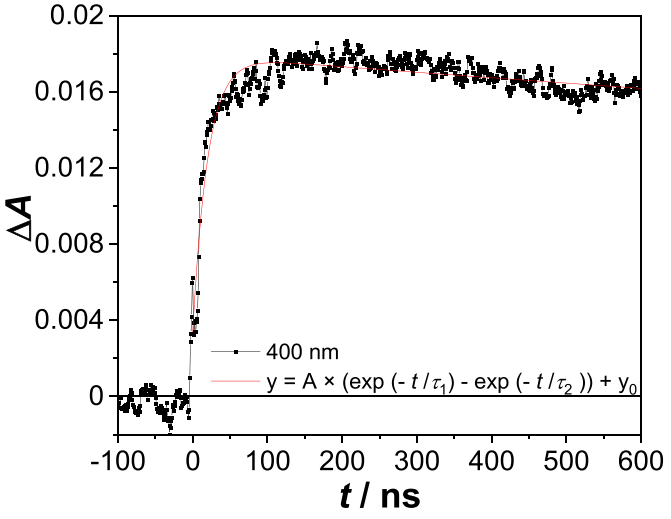

Fig. 4. Buildup of the transient monitored at 400 nm after the laser pulse of N_2-saturated CH_3CN solution of HPT (0.1 mM) and ROSU (0.75 mM). $E_{355\ nm} \approx 5$ mJ.

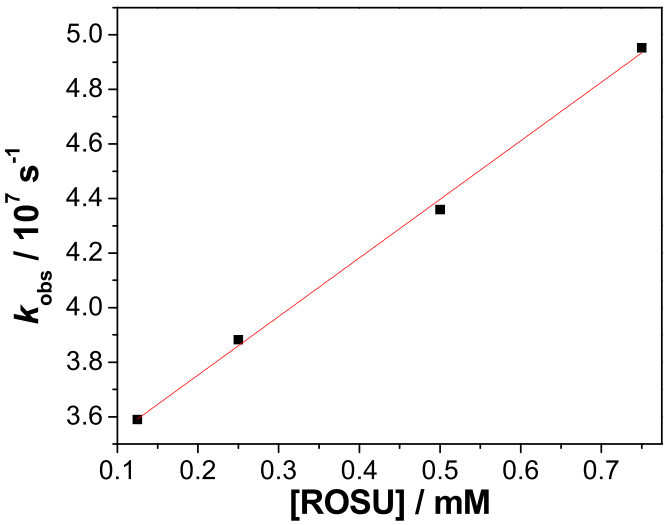

Fig. 5. Plot according to equation (3) for the buildup of the transient monitored at 400 nm after the laser pulse of N_2-saturated CH_3CN solution of HPT (0.1 mM) containing different concentrations of ROSU.

constant k_R is calculated to be $(2.15 \pm 0.07) \times 10^{10}\ M^{-1}\ s^{-1}$ (Fig. 5). The obtained lifetime of the •OH radicals in the absence of ROSU, $\tau_0 = 30$ ns, is in a good agreement with the literature value obtained for •OH radicals formed *via* HPT photolysis in the reaction with *trans*-stilbene (De Matteo et al., 2005).

The determined rate constant, k_R is slightly higher than the maximum value of the diffusion controlled rate constant of aromatic molecules with •OH radicals (Wojnárovits and Takács, 2013) and it is in accordance with reactions of other statins with •OH radicals in H_2O, whose previously published second-order rate constants are summarized in Table 2. In order to propose the most preferable pathway of ROSU reaction with •OH radicals and to identify radiolytic products, MS/MS analysis is introduced.

3.3. Identification of ROSU degradation products

The main radiolytic products of ROSU samples irradiated in air were identified, seven of which are new compared to ROSU degradation under oxidative conditions: **C1**–**C3**, **C5**–**C6**, **C11** and **C16** (Scheme 2). Hydroxylation on the fluorobenzene ring of ROSU is the most pronounced with the formation of **C8**–**C10** and **C12**–**C13**, and these products were also identified after irradiation of ROSU under oxidative conditions (Dončević et al., 2021). These results are in accordance with

Table 2
Second-order rate constants for the reaction of different statins with •OH radicals.

Statin	Method	Solvent	k_{OH} ($M^{-1}\ s^{-1}$)
Atorvastatin	UV photolysis	Phosphate buffer (pH = 7)	$(1.19 \pm 0.05) \times 10^{10}$ (Razavi et al., 2011a)
	Simulated solar photolysis		
	Simulated solar photolysis	Synthetic field water	$(1.9 \pm 0.5) \times 10^{10}$ (Lam and Mabury, 2005)
Fluvastatin	Pulse radiolysis	Phosphate buffer (pH = 7)	$(6.96 \pm 0.16) \times 10^9$ (Razavi et al., 2011b)
Simvastatin			$(3.14 \pm 0.15) \times 10^9$ (Razavi et al., 2011b)
Pravastatin			$(4.16 \pm 0.13) \times 10^9$ (Razavi et al., 2011b)
Lovastatin			$(2.92 \pm 0.06) \times 10^9$ (Razavi et al., 2011b)
Rosuvastatin	**Laser flash photolysis**	**CH_3CN**	**$(2.15 \pm 0.07) \times 10^{10}$ (our work)**

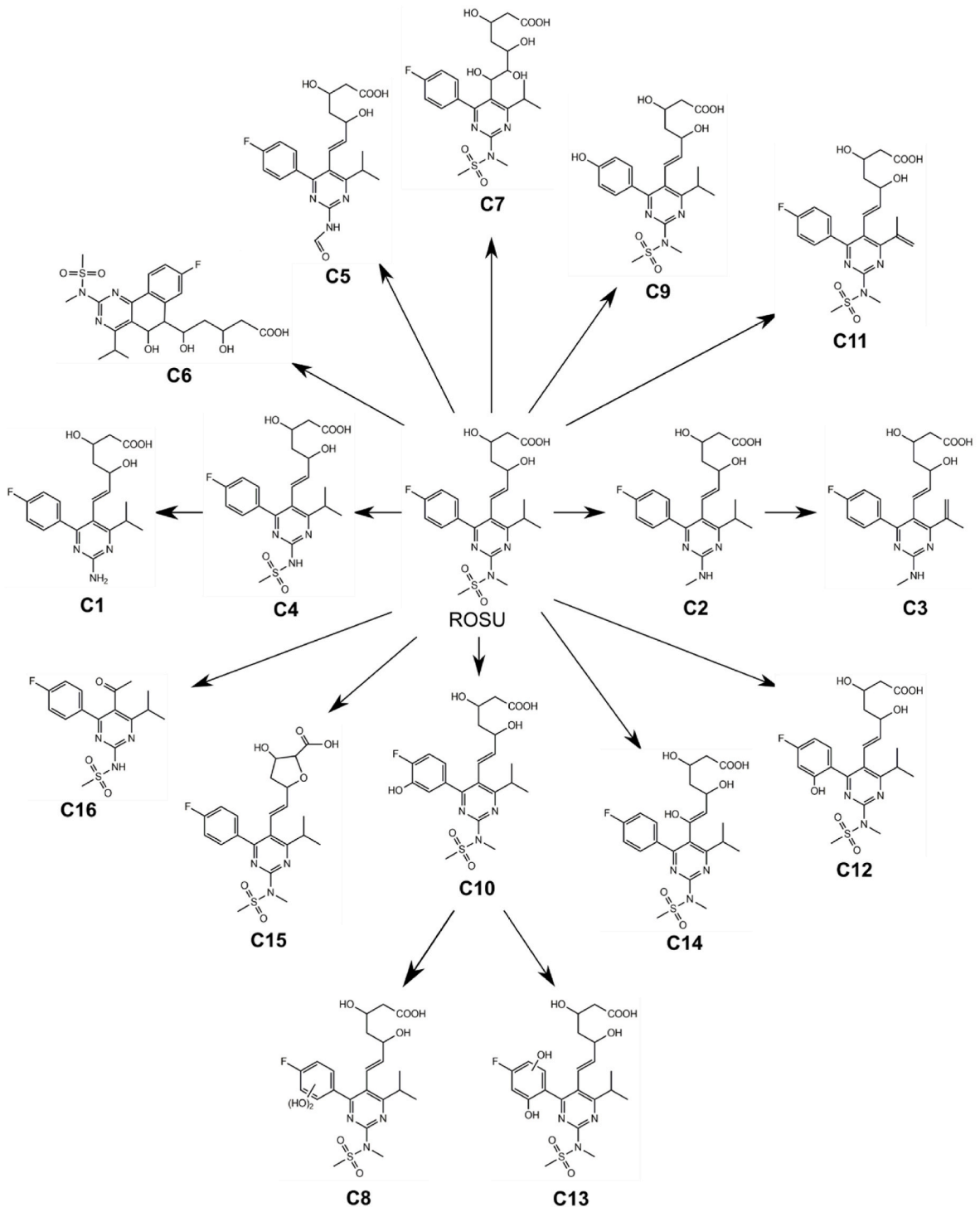

Scheme 2. Products obtained after γ-radiolysis (D = 1000 Gy, dD/dt = 4.93 Gy s^{-1}) of buffered solution (pH ≈ 6.8) of ROSU (0.1 mM) in equilibrium with air. **C1–C3**, **C5–C6**, **C11** and **C16** are newly-identified compounds.

the results of laser flash photolysis, as they confirm the formation of a new transient as a result of the reaction of ROSU with $^{\bullet}$OH radicals. Hydroxylation is also observed at the double bond of the hept-6-enoic acid side chain with the formation of **C7** and **C14** (Segalin et al., 2015).

The proposed structures of the found degradation products are shown in Scheme 2, while in Tables S1–S19 and Schemes S1-S17 the results of MS/MS analysis are presented. The structures of the newly observed ROSU degradation products as well as the previously identified products were suggested based on their MS/MS.

The **C1–C4** structures were the result of cleavage of the methyl and/or methyl sulfonyl group, which can be seen from the absence of fragment ions at m/z 421 and 378, instead of which fragment ions at m/z 330 and 286 (**C1**), m/z 421 and 300 (**C2**) and at m/z 342 and 298 (**C3**) were observed. Based on the MS/MS spectra, **C4** was identified as *N*-desmethyl rosuvastatin, a known rosuvastatin metabolite (Bai et al., 2018).

Four degradation products (**C6**, **C10**, **C12** and **C14**) with the same exact mass of m/z 498 were observed at different retention times, but based on their fragmentation pathways, their different structures could be suggested. The main difference lies in the position of the additional

hydroxyl group that can be bound to the fluorobenzene ring or to the double bond of hept-6-enoic acid side chain. Hydroxylation of the fluorobenzene ring leads to the formation of **C10** and **C12**, while hydroxylation of the double bond leads to formation of **C6** and **C14**, with cyclization occurring during the formation of **C6**.

The formation of dihydroxylated ROSU was also observed. Compounds **C8** and **C13**, observed at retention times of 7.1 and 8.0 min, respectively, have similar structures, where both hydroxyl groups are bound to the fluorobenzene ring. However, due to the higher retention time of **C13**, the position of one hydroxyl group can be determined, since it is known that the formation of intramolecular bonds decreases the solute-solvent association, causing longer retention times due to the stronger solute-stationary phase association (Clark et al., 1988; Fitch et al., 2018). Compound **C7,** on the other hand, is formed by hydroxylation of the double bond, as the ions *m/z* 270, 256, and 258, which were also found in the MS/MS spectra of ROSU and are characteristic for fluorobenzene ring, were observed.

In a previous study, ROSU irradiation was investigated under oxidative conditions (Dončević et al., 2021). In this study, irradiation was performed in air-saturated samples. There is a significant difference in the results obtained, as irradiation in the presence of air resulted to the formation of a greater variety of degradation products. Even though the main reaction pathway is hydroxylation, leading to the formation of various hydroxylated and dihydroxylated degradation products, other types of reactions also take place, as can be seen in **C3** for example. These reactions can be attributed to the presence of the reductive reactive species $H^{\bullet}$ and e^{-}_{aq}, which initially react with both ROSU and oxygen present in air-saturated aqueous solution, depending on all competing rate constants involved, the known concentration of oxygen (0.25 mM) in water, and the ROSU concentration used (0.1 mM).

4. Conclusions

ROSU was found to be easily susceptible to degradation under the influence of ionizing radiation. Our results showed that γ-irradiation can be used as an effective method for removing ROSU from wastewater. Seven new radiolytic products were identified by irradiation of aqueous ROSU solutions in equilibrium with air compared to ROSU degradation under oxidative conditions. The high value of the determined rate constant of the reaction of ROSU and $^{\bullet}$OH radicals, $2.15 \pm 0.07 \times 10^{10}$ M^{-1} s^{-1}, and the identified radiolytic products suggest that hydroxylation is the most preferable pathway of ROSU degradation. The most favorable position for hydroxylation is at the fluorobenzene ring of ROSU. Similar radiolytic products could be expected for other statins subjected to γ-irradiation in air.

Authorship statement

Category 1
Conception and design of study: I. Dz
acquisition of data: L. M., M. P.
analysis and/or interpretation of data: L. M, M. P, N. G, B. M., I. Dz.
Category 2
Drafting the manuscript: L. M, M. P.
revising the manuscript critically for important intellectual content: N. G., B. M. I. Dz.
Category 3
Approval of the version of the manuscript to be published (the names of all authors must be listed):
Leo Mandić, Marijana Pocrnić, Nives Galić, Branka Mihaljević, Iva Džeba

Declaration of competing interest

The authors declare that they have no known competing financial interests or personal relationships that could have appeared to influence the work reported in this paper.

Data availability

Data will be made available on request.

Acknowledgements

The authors thank Dr. Irena Ciglenečki-Jušić, Division for Marine and Environmental Research, Ruđer Bošković Institute, for the TOC measurements.

The support and cooperation with the IAEA in the RER1021 regional project are kindly acknowledged. The authors also acknowledge the support of the CIuK project co-financed by the Croatian Government and the European Union through the European Regional Development Fund-Competitiveness and Cohesion Operational Programme (Grant KK.01.1.1.02.0016.).

Appendix A. Supplementary data

Supplementary data to this article can be found online at https://doi.org/10.1016/j.radphyschem.2023.110885.

References

Akhtar, J., Amin, N.A.S., Shahzad, K., 2015. A review on removal of pharmaceuticals from water by adsorption. Desalination Water Treat. 57, 12842–12860.
Aveline, B.M., Kochevar, I.E., Redmond, R.W., 1996. Photochemistry of the nonspecific hydroxyl radical generator, *N*-hydroxypyridine-2(1*H*)-thione. J. Am. Chem. Soc. 118, 10113–10123.
Azemawah, V., Movahed, M.R., Centuori, P., Penaflor, R., Riel, P.L., Situ, S., Shadmehr, M., Hashemzadeh, M., 2019. State of the art comprehensive review of individual statins, their differences, pharmacology, and clinical implications. Cardiovasc. Drugs Ther. 33, 625–639.
Bai, X., Wang, X.-P., He, G.-D., Zhang, B., Huang, M., Li, J.-L., Zhong, S.-L., 2018. Simultaneous determination of rosuvastatin, rosuvastatin-5S-lactone, and *N*-desmethyl rosuvastatin in human plasma by UPLC-MS/MS and its application to clinical study. Drug Res. 68, 328–334.
Buxton, G.V., Greenstock, C.L., Helman, W.P., Ross, A.B., 1988. Critical review of rate constants for reactions of hydrated electrons, hydrogen atoms and hydroxyl radicals ($^{\bullet}$OH/$^{\bullet}$O^{-}) in aqueous solution. J. Phys. Chem. Ref. Data 17, 513–886.
Cheng, J.W.M., 2004. Rosuvastatin in the management of hyperlipidemia. Clin. Therapeut. 26, 1368–1387.
Clark, M.R., Garcia-Roura, L.E., Clark, C.R., 1988. Intramolecular hydrogen bonding effects on the reversed-phase retention of substituted acetophenones. J. Liq. Chromatogr. 11, 3213–3221.
Coimbra, R.N., Escapa, C., Otero, M., 2021. Removal of pharmaceuticals from water: conventional and alternative treatments. Water 13, 487.
Cuerda-Correa, E.M., Alexandre-Franco, M.F., Fernández-González, C., 2019. Advanced oxidation processes for the removal of antibiotics from water. An Overview. Water 12, 102.
Dautović, J., Vojvodić, V., Tepić, N., Ćosović, B., Ciglenečki, I., 2017. Dissolved organic carbon as potential indicator of global change: a long-term investigation in the northern Adriatic. Sci. Total Environ. 587–588, 185–195.
De Matteo, M.P., Poole, J.S., Shi, X., Sachdeva, R., Hatcher, P.G., Hadad, C.M., Platz, M. S., 2005. On the electrophilicity of hydroxyl radical: a laser flash photolysis and computational study. J. Am. Chem. Soc. 127, 7094–7109.
Demasi, M., 2018. Statin wars: have we been misled about the evidence? A narrative review. Br. J. Sports Med. 52, 905–909.
Dončević, L., Svetličić, E., Hozić, A., Mihaljević, B., Jarmuzek, D., Tartaro Bujak, I., Pluskota-Karwatka, D., Ozdanovac, L., Džeba, I., Cindrić, M., 2021. NanoUPLC-QTOF-MS/MS Determination of major rosuvastatin degradation products generated by gamma radiation in aqueous solution. Pharmaceuticals 14, 1160.
Fitch, W.L., Khojasteh, C., Aliagas, I., Johnson, K., 2018. Using LC retention times in organic structure determination: drug metabolite identification. Drug Metabol. Lett. 12, 93–100.
Gadipelly, C., Pérez-González, A., Yadav, G.D., Ortiz, I., Ibáñez, R., Rathod, V.K., Marathe, K.V., 2014. Pharmaceutical industry wastewater: review of the technologies for water treatment and reuse. Ind. Eng. Chem. Res. 53, 11571–11592.
Golovko, O., Kumar, V., Fedorova, G., Randak, T., Grabic, R., 2014. Seasonal changes in antibiotics, antidepressants/psychiatric drugs, antihistamines and lipid regulators in a wastewater treatment plant. Chemosphere 111, 418–426.
Iglesias, P., Díez, J.J., 2003. New drugs for the treatment of hypercholesterolaemia. Expet Opin. Invest. Drugs 12, 1777–1789.
Jones, R.A., Katritzky, A.R., 1960. *N*-Oxides and related compounds. Part XVII. The tautomerism of mercapto- and acylamino-pyridine 1-oxides. J. Chem. Soc. 2937–2942.

Kanakaraju, D., Glass, B.D., Oelgemöller, M., 2018. Advanced oxidation process-mediated removal of pharmaceuticals from water: a review. J. Environ. Manag. 219, 189–207.

Lam, M.W., Mabury, S.A., 2005. Photodegradation of the pharmaceuticals atorvastatin, carbamazepine, levofloxacin, and sulfamethoxazole in natural waters. Aquat. Sci. 67, 177–188.

Lee, H.B., Peart, T.E., Svoboda, M.L., Backus, S., 2009. Occurrence and fate of rosuvastatin, rosuvastatin lactone, and atorvastatin in Canadian sewage and surface water samples. Chemosphere 77, 1285–1291.

Luvai, A., Mbagaya, W., Hall, A.S., Barth, J.H., 2012. A review of the pharmacology and clinical effectiveness in cardiovascular disease. Clin. Med. Insights Cardiol. 6, 17–33.

Machado, T.C., Pizzolato, T.M., Arenzon, A., Segalin, J., Lansarin, M.A., 2015. Photocatalytic degradation of rosuvastatin: analytical studies and toxicity evaluations. Sci. Total Environ. 502, 571–577.

Majer, M., Roguljić, M., Knežević, Z., Starodumov, A., Ferenček, D., Brigljević, V., Mihaljević, B., 2019. Dose mapping of the panoramic ^{60}Co gamma irradiation facility at the Ruđer Bošković Institute - geant4 simulation and measurements. Appl. Radiat. Isot. 154, 108824.

Massima Mouele, E.S., Tijani, J.O., Badmus, K.O., Pereao, O., Babajide, O., Zhang, C., Shao, T., Sosnin, E., Tarasenko, V., Fatoba, O.O., Laatikainen, K., Petrik, L.F., 2021. Removal of pharmaceutical residues from water and wastewater using dielectric barrier discharge methods - a review. Int. J. Environ. Res. Publ. Health 18, 1683.

Razavi, B., Ben Abdelmelek, S., Song, W., O'Shea, K.E., Cooper, W.J., 2011a. Photochemical fate of atorvastatin (lipitor) in simulated natural waters. Water Res. 45, 625–631.

Razavi, B., Song, W., Santoke, H., Cooper, W.J., 2011b. Treatment of statin compounds by advanced oxidation processes: kinetic considerations and destruction mechanisms. Radiat. Phys. Chem. 80, 453–461.

Ražem, D., Dvornik, I., 1987. Ethanol-chlorobenzene dosimetry for absorbed doses below 1 kGy. Appl. Radiat. Isot. 38, 1019–1025.

Segalin, J., Sirtori, C., Jank, L., Lima, M.F., Livotto, P.R., Machado, T.C., Lansarin, M.A., Pizzolato, T.M., 2015. Identification of transformation products of rosuvastatin in water during ZnO photocatalytic degradation through the use of associated LC-QTOF-MS to computational chemistry. J. Hazard Mater. 299, 78–85.

Spinks, J.W.T., Woods, R.J., 1990. An Introduction to Radiation Chemistry, third ed. John Wiley & Sons, Inc., Toronto.

Sulaiman, S., Khamis, M., Nir, S., Lelario, F., Scrano, L., Bufo, S.A., Mecca, G., Karaman, R., 2015. Stability and removal of atorvastatin, rosuvastatin and simvastatin from wastewater. Environ. Technol. 36, 3232–3242.

Wang, J., Wang, S., 2016. Removal of pharmaceuticals and personal care products (PPCPs) from wastewater: a review. J. Environ. Manag. 182, 620–640.

Wojnárovits, L., Takács, E., 2013. Structure dependence of the rate coefficients of hydroxyl radical + aromatic molecule reaction. Radiat. Phys. Chem. 87, 82–87.